Environmental Research 298 (2026) 124221

Contents lists available at ScienceDirect

Environmental Research

journal homepage: www.elsevier.com/locate/envres

Distance decay of tire wear particles and potentially toxic elements near Canada's busiest highway: Assessing lichen transplants as biomonitors

Lisa Grifoni [a,b], Aldo Winkler [b], Mehriban Jafarova [c], Lilla Spagnuolo [b], Julian Aherne [c,*], Stefano Loppi [a]

[a] Department of Life Sciences, University of Siena, Italy
[b] Istituto Nazionale di Geofisica e Vulcanologia, Rome, Italy
[c] School of Environment, Trent University, Peterborough, ON, K9L 0G2, Canada

A B S T R A C T

Non-exhaust emissions from road traffic, including tire wear particles (TWPs), potentially toxic elements (PTEs), and magnetic metallic particles (MMPs), represent an emerging component of urban air pollution. Here we evaluated the suitability of lichen transplants (*Evernia prunastri*) as a biomonitor of TWPs, PTEs and MMPs along a 150 m transect from Highway 401, Toronto, Ontario (Canada). Lichens were exposed for 2 months at six different distances from the highway and analysed for TWPs, PTEs, and MMPs. Lichen transplants showed an exponential decrease in the accumulation of TWPs with distance from the highway (estimated at >17,500 to ~1500 TWP g^{-1}; $R^2 = 0.98$). The concentration of Sb and MMPs, the latter deduced by magnetic susceptibility values, declined sharply (by 70%) within 35 m of the road, while most other PTEs decreased by 50% at 150 m. The strong associations between TWPs and non-exhaust tracers (Sb, Cr, and MMPs; r = 0.69, 0.68, and 0.83, respectively) indicate a shared traffic-related source arising from combined tire and brake wear and highlight the potential of magnetic susceptibility as a rapid proxy for assessing the dispersion of TWPs.

1. Introduction

Traffic emissions are a major contributor to atmospheric pollution, releasing complex mixtures of particulate matter, including magnetic metallic particles (MMPs), potentially toxic elements (PTEs), and non-exhaust emissions. The latter originate from brakes, tires, erosion of road surfaces, and resuspension of a mixture of road dust, which pose significant threats to the environment (Gulia et al., 2015; Boucher and Friot, 2017; Demková et al., 2019).

In recent decades, the increase in the number of road vehicles has raised concerns about air quality along heavily trafficked highways, especially those that traverse metropolitan areas. Indeed, non-exhaust emissions pose a risk both from an environmental perspective and in terms of their impact on human health (Fussell et al., 2022; Amato et al., 2014). For this reason, a wide range of studies have been conducted in urban settings, e.g., in Turku, Finland, one study assessed stop-and-go traffic-induced particulate matter (PM) using moss bags (Limo et al., 2018), in Milan, Italy, magnetic particulates were assessed using lichen bags (Winkler et al., 2020) and in London, UK, non-exhaust emissions sources have been assessed (Hicks et al., 2021).

Tire wear particles significantly contribute to global microplastic (MP) pollution, with annual tire wear particle (TWP) emissions estimated at approximately 6,000,000 tons (Kole et al., 2017). As a result, tire abrasion is one of the main sources of MP dispersion globally (Hartmann et al., 2019). Tires are typically composed of blends of natural and synthetic rubber, supplemented with additives such as sulfur, zinc oxide, and reinforcing agents like carbon black or silica (Kole et al., 2017). The contribution of TWPs to environmental MPs varies considerably, reaching up to 93% in areas close to major highways (Giechaskiel et al., 2024), and it is predicted to increase with the use of electric vehicles (Foroutan et al., 2025). Furthermore, friction between tires and road surfaces may generate complex TWPs containing embedded metallic particles, predominantly originating from brake wear and from the internal frame of the tire, along with organic and mineral materials from road surface abrasion (Panko et al., 2018). These processes can yield larger, structurally intricate particle aggregates (Dall'Osto et al., 2014).

Biomonitoring using living organisms is a valuable and sustainable approach for assessing the relative levels of airborne pollutants, as well as their diffusion patterns (Parmar et al., 2016; Theophilo et al., 2021). Lichens are especially suitable for this purpose owing to their unique physiological characteristics (Conti and Cecchetti, 2001). The use of

This article is part of a special issue entitled: Biomonitoring environmental pollution published in Environmental Research.

* Corresponding author.
E-mail address: jaherne@trentu.ca (J. Aherne).

https://doi.org/10.1016/j.envres.2026.124221
Received 20 November 2025; Received in revised form 17 February 2026; Accepted 6 March 2026
Available online 6 March 2026

lichen transplants, i.e., lichens collected from a remote area and exposed for a given time period in the area of investigation, has gained recognition for biomonitoring in urban areas devoid of lichens or where the lichen flora is scarce, offering practical and cost-effective advantages (Loppi and Paoli, 2015). Transplants of the fruticose lichen *Evernia prunastri* (L.) Ach. have been extensively used for monitoring of MMPs and PTEs from traffic emissions (Winkler et al., 2020). This approach has been successfully applied to biomonitor the deposition of airborne MPs in urban environments (Grifoni et al., 2025a).

Although the use of lichens as biomonitors of atmospheric pollution is well established, their application for monitoring TWPs remains largely unexplored. In particular, previous biomonitoring studies have focused on airborne MPs such as microfibres, providing limited information on the potential of lichens to capture and spatially resolve TWPs emitted from road traffic, especially in proximity to major highways. Moreover, to the best of our knowledge, no studies have jointly investigated TWPs, PTEs and MMPs to characterize non-exhaust traffic emissions using a lichen transplant approach. To address these knowledge gaps, this study evaluated the suitability of *E. prunastri* transplants as biomonitors of airborne TWPs emitted by road traffic. Specifically, we investigated the spatial distribution of TWPs along a 150 m transect from Highway 401 in Toronto, Ontario, Canada, which is the busiest highway of North America, accommodating up to 450,000 vehicles daily as it traverses the Greater Toronto Area. Yet no studies have assessed the atmospheric dispersion of particulate mixtures from Highway 401. In parallel, the accumulations of PTEs and MMPs were assessed and used as a proxy for non-exhaust traffic-related emissions. This study provides the first field-based assessment of the capacity of lichen transplants to biomonitor airborne TWPs in a high-traffic highway environment, offering a spatially resolved analysis of TWP dispersion at different distances. By jointly analyzing TWPs, PTEs and MMPs, this work presents an integrated characterization of non-exhaust traffic emissions, advancing our current understanding of their composition and dispersion patterns in urban environments.

2. Methods

2.1. Study area

Our study was conducted along a 150 m transect roughly perpendicular to Highway 401 at Resources Road (43.7109, −79.5476) in Etobicoke, which is a suburb in the western part of the City of Toronto (Ontario, Canada), from the 5th of June to the 5th of August, 2025 (61 days). Highway 401 had an annual average daily traffic of 424,600 vehicles in 2021 (Ministry of Transportation of Ontario [MTO], 2021). However, during peak hours, traffic congestion frequently results in stationary vehicles. The region experiences a humid continental climate-type, with warm, humid summers and cold, snowy winters. Rainfall during the exposure period was 170.4 mm, with 14 rainy days and only one event of rain during the last ten days of exposure; the mean temperature was 21.1 °C and mean wind speed was 4 m s^{-1} (ECCC, 2020).

2.2. Lichen bag deployment

The lichen *Evernia prunastri* (L.) Ach. was selected as a biomonitor owing to its characteristics, such as its wide surface area and its ability to collect both PTEs and MPs (Loppi et al., 1998; Cercasov et al., 2002; Jafarova et al., 2023). Thalli were harvested in June 2025 from Warsaw Caves Conservation Area (44.4578, −78.1278, 240 m a.s.l.), a rural background site in Ontario, which has been used in previous studies (Bertrim and Aherne, 2023; Jafarova and Aherne, 2026) as it is located far from urban settlements and human activity. In the laboratory, samples were roughly cleaned of debris, air dried, and thalli (about 2 g) were then wrapped in a square plastic net (20 × 20 cm) with a mesh size of 8 × 8 mm; the net was green and its composition, tested analytically with μ-FT-IR, was made up of high density polyethylene (HDPE). A bagging net was used to avoid the loss of lichen material; further, we choose HDPE rather than metal mesh, to avoid potential contamination of samples with PTEs through direct contact, and also because its color and known composition made any possible sample contamination easy to detect. However, we are aware that electrostatic effects may have potentially caused plastic particles to accumulate to the net due to static charge, since HDPE easily accumulates and retains electrostatic charges, but this may be less likely to influence TWPs. On the 5th of June, 18 lichen bags were exposed (in triplicate at each of the six sites) on lamp posts or wooden hydro poles along a transect located at distances of about 5, 10, 35, 70, 100 and 150 m roughly perpendicular from Highway 401; further, five bags were kept as unexposed controls in paper bags, making 23 lichen bags in total. Sites for deployment were chosen to reflect increasing distances from Highway 401 and to guarantee unhindered airflow in order to evaluate the dispersion range of non-exhaust particles and also based on the availability of aligned posts. The lichen bags were attached to fence, hydro or lamp posts using zinc-plated L brackets at a height of about 2 m above ground. On the 5th of August, all lichen bags were collected and stored individually in paper bags prior to analysis.

2.3. Tire wear particle extraction

From each lichen bag (n = 23), 1 g of material was air dried and digested using a wet peroxide oxidation method (Roblin and Aherne, 2020; Loppi et al., 2021; Jafarova et al., 2023). Samples were then vacuum-filtered onto glass-fibre filter papers (Fisherbrand Glass Fibre G6, Ø 1.6 μm) and placed into glass Petri dishes before further analysis. The filter papers were examined for TWPs under a stereomicroscope (AmScope) equipped with a digital camera (MU1000), visual analysis was limited to >50 μm. Each particle was visually assessed as a TWP and manually tested using four identification criteria: (1) black in colour, (2) elongated in shape, (3) rough surface texture, and (4) spongy when poked with a needle but remained intact (Leads and Weinstein, 2019).

2.4. Quality control

Procedures to ensure the absence of contamination were followed. All the reagents and solution, including Reverse Osmosis water, were vacuum filtered before their usage in MP extraction. Plastic utensils were avoided and cotton clothes were used by the operators. Analytical blanks were performed in order to evaluate potential laboratory contamination, however, no TWPs were detected in blanks.

2.5. Tire wear particle estimation

Direct counting of TWPs exceeded the threshold for reliable manual counting (>500 TWP g^{-1} dw) due to the very high number of particles; concentrations for each sample were therefore estimated using standardized subsampling and extrapolation protocols, which have been widely used in microplastic analysis (Allen et al., 2019; Brandt et al., 2021). Each digested sample (1 g) was filtered sequentially using three separate paper filters: one for the initial half of the digestion solution, a second for the remaining half, and a third for the final rinse (three filtration levels per replicate A, B, C; Fig. 1). The surface area of the digested lichen residue on each filter was measured by quantifying the digestion residue ring area, as the mean of 20 measurements from different filters for each filtration step, namely 2454 mm^2 for the first step, 2221 mm^2 for the second step, 1963 mm^2 for the third filtration step (Fig. 1). Within the brownish residue ring of each filter, three randomly selected areas (2.4 mm^2 each) were photographed under a stereomicroscope at 4× magnification. In each area, the TWPs were identified and counted (size LOD >50 μm), and the number of TWPs in 2.4 mm^2 was calculated as the mean of three areas for each filter. The total number of TWPs on each filter was then extrapolated to the

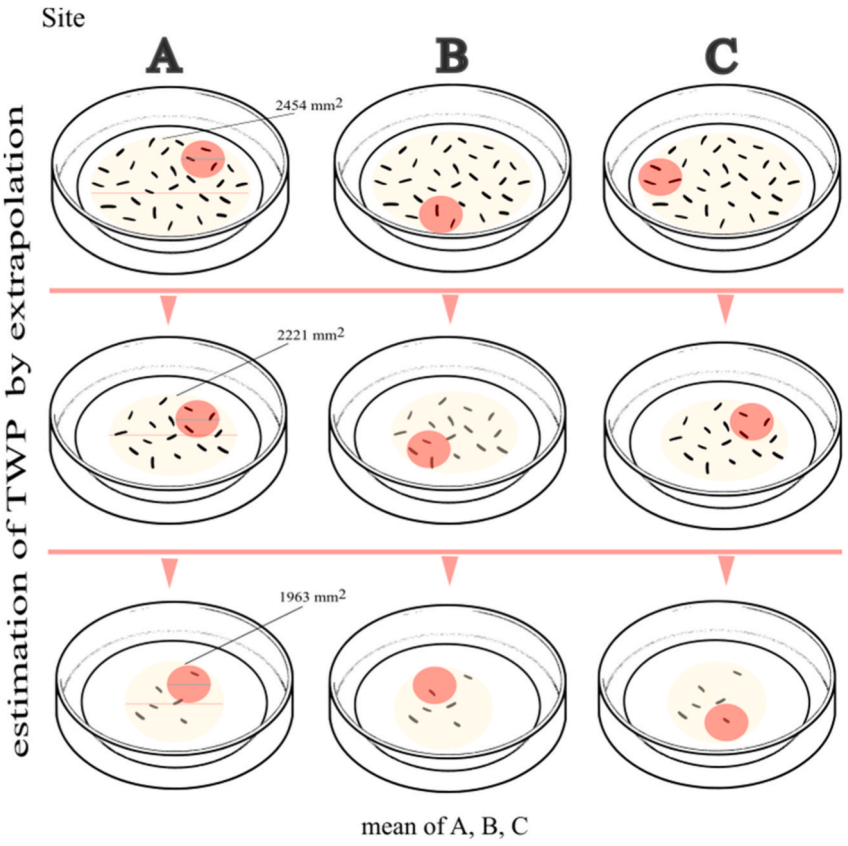

Fig. 1. Estimation of tire wear particles (TWP) for each site was carried out in three steps for each biological replicate: (1) count of TWPs in three random areas of fixed size (red circles) within the lichen digested area and extrapolation to the entire filter (specified area for each step of filtration), (2) sum of the count for each petri of a replicate (n = 3 in column), and (3) mean of total count for each replicate (A, B, C, n = 3).

brownish digestion ring area, for the first, second, and third step, respectively. Finally, the estimated amounts from each step were summed to obtain an estimate of the total TWP content per replicate. The TWP content for each site was calculated as the mean of three replicates deployed at each transect site.

2.6. Tire wear particle characterization

The polymer characterization was performed on a randomly selected 5% subsample of suspected TWPs using micro-Fourier Transform Infrared spectroscopy (μ-FTIR, LUMOS II, Bruker Scientific LLC, Germany) in attenuated total reflectance (ATR) mode. Prior to analysis, isolated TWPs were placed onto glass slides lined with double-sided tape, arranged systematically in rows, and each particle position was recorded with an individual identifier. The prepared slides were then positioned onto the μ-FTIR stage for analysis. Spectra were acquired over a wavenumber range of 400–4000 cm^{-1} by averaging 32 scans per particle using LUMOS II OPUS spectroscopy software (version 8.7.31). Before each measurement, the ATR crystal was cleaned with isopropyl alcohol to avoid cross-contamination. Three replicate spectra were obtained for each particle to ensure spectral quality and reproducibility. Particle spectra were subsequently identified using the open-source spectral database Open Specy (openanalysis.org/openspecy; Cowger et al., 2021). The best spectral match was selected based on achieving a Pearson correlation coefficient higher than 0.70. The total TWP count estimates were corrected for the percentage of mineral or organic matter identified by μ-FTIR analysis: notably 48% for Site 1, 39% for Site 2, 23% for Site 3, 8% for Site 4, 13% for Site 5 and 50% for Site 6. Furthermore, measurements of particle length and width carried out using ImageJ were used to calculate the ellipsoid volume of each TWP. Subsequently, TWP mass concentration (μg g^{-1} dw) per sampling site was estimated by summing the product of particle volume by polymer density, according to the following formula:

mass (μg g^{-1} dw) = (volume (cm^3) × density (g cm^{-3}) × 10^6) / mass of lichen (g dw)

2.7. Trace element analysis

Lichen thalli were carefully cleaned and then air dried, homogenized, and analysed for nine PTEs (Al, Ba, Cd, Cr, Cu, Fe, Mn, Sb and Zn). For each replicate, 250 mg of lichen thalli was acid digested with a mixture of 3 mL HNO_3 (70 %), 0.2 mL HF, and 0.5 mL H_2O_2 using a microwave digestion system (Ethos 900, Milestone, Bergamo, Italy). The PTEs were detected by ICP-MS (NexION 350, PerkinElmer, Waltham, MA, USA). Analytical quality was checked using procedural blanks and the certified reference materials, IAEA336 “Lichen” and GBW07604 “Poplar leaves”. Recoveries ranged 91–113%; accuracy, expressed by the relative standard deviation of three replicates, was below 3 % for all elements.

2.8. Magnetic analysis

The mass magnetic susceptibility (χ) of each replicate was determined through an Agico KLY5 meter, normalizing for the mass of the samples placed inside 8 cm^3 paleomagnetic plastic cubes, under a magnetic field of 400 A/m (1220 Hz). The hysteresis properties, including coercive force (Bc), remanent coercivity (Bcr), saturation remanent magnetization by mass (Mrs), and saturation magnetization by mass (Ms), were measured on randomly selected sample fragments placed inside #4 pharmaceutical gel caps using a Lakeshore 8604

vibrating sample magnetometer (VSM) at a maximum applied field of 1.0 T. The values were calculated by first subtracting the high-field paramagnetic linear trend and then dividing the corrected magnetic moments by the net sample mass. The coercivity of remanence (Bcr) values were interpolated from backfield remagnetization curves up to −1 T, after saturating at 1 T field. The domain state and magnetic grain-size of the samples were compared to theoretical magnetite according to the hysteresis ratios Mrs/Ms *vs* Bcr/Bc in the "Day plot" (Day et al., 1977; Dunlop, 2002a, 2002b). First-order reversal curve (FORC) diagrams were used for outlining the interaction field (Bu) and coercivity distributions in selected samples, to disentangle the single domain (SD), multidomain (MD) and pseudo-single domain/vortex (PSD/V) behaviors (Pike et al., 1999; Roberts et al., 2000). FORCs were measured at steps of 2.5 mT, with 300 ms averaging time and maximum applied field 1.0 T. The diagrams were processed, Variforc smoothed (up to 10 at the ridges and to 14 at the background due to the weak magnetic properties) and drawn with the FORCINEL 3.08 Igor Pro routine (Harrison and Feinberg, 2008).

2.9. Statistical analysis

The normality of the variables was assessed using the Shapiro–Wilk test ($p < 0.05$). Where skewed distributions were observed, i.e., for Fe, χ, and Sb, data were log-transformed prior to statistical analysis. Correlations were calculated using the Pearson correlation coefficient ($p < 0.05$). The relationship of TWPs, PTEs and MMPs with distance from the highway was modelled using a non-linear exponential decay function fitted by non-linear least squares ($p < 0.05$). Uncertainty of parameters was quantified using 95% confidence intervals. Average daily TWP deposition rate was estimated using a lichen mass/surface area ratio of 0.012 $m^2\ g^{-1}$ (Grifoni et al., 2025a) and the exposure time of 61 days. All calculations were run using R (R Core Team, 2025).

3. Results

3.1. Tire wear particles

The content of TWPs in unexposed lichens was <10 and was regarded as negligible. In contrast, exposed samples accumulated TWPs all along the 150 m transect (Table 1). The highest number of TWPs was found at site 2, while the highest TWP mass was found at site 1; Site 6 was the lowest in terms of both number and mass. (Table 1).

The mass of TWP accumulated by lichen transplants decreased exponentially with distance from the highway (Fig. 2).

The average daily TWP deposition ranged from 2054 particles $m^{-2}d^{-1}$ (site 6) to 40,464 particles $m^{-2}d^{-1}$ (site 2), with an average of 18,656 particles $m^{-2}d^{-1}$. By mass, TWP deposition decreased from 2348 μg $m^{-2}d^{-1}$ (site 1) to 34 μg $m^{-2}d^{-1}$ (site 6), with an average of 787 μg $m^{-2}d^{-1}$. Particle length was independent of the distance from the highway and spanned over a range of >800 μm; across the transect, the dominant dimension range (>50%) was 50–100 μm (Fig. 3).

Among the synthetic polymers, Polypropylene (PP), Polymethylmethacrylate (PMMA) and rubber were the most common, notably 28%, 20% and 17%, respectively. However, other polymers were identified: Polyethylene Terephthalate (PET; 13%), Polyvinyl Chloride (PVC; 11%), Polyethylene (PE; 9%), paint (2%) and Low-Density Polyethylene (LDPE; 1%).

Table 1
Tire wear particles (TWPs) accumulated by lichen transplants (mean ± standard error) by number and by mass at each study site (see text). The minimum, maximum, and mean (± standard error) length of TWP are also shown.

	Site 1	Site 2	Site 3	Site 4	Site 5	Site 6
Number (n g^{-1}, dw)	17543 ± 1365	29620 ± 2983	19551 ± 1564	9268 ± 166	4453 ± 566	1504 ± 430
Mass (μg g^{-1}, dw)	1719 ± 720	800 ± 148	498 ± 149	285 ± 108	129 ± 39	25 ± 10
Mean length (μm)	99 ± 8	84 ± 8	72 ± 3	88 ± 6	75 ± 5	91 ± 6
Min length (μm)	29	25	24	33	35	49
Max length (μm)	239	840	239	326	181	150

3.2. Potentially toxic elements

Lichen samples exposed close to the highway accumulated relatively high amounts of all PTEs except for Al (Table 2).

The accumulation of Sb was particularly severe, with up to a 26-fold increase compared with unexposed samples; furthermore, it showed an exponential decrease with distance from the highway ($R^2 = 0.96$, $p < 0.05$). The accumulation of Fe also decreased exponentially with distance from the highway ($R^2 = 0.94$, $p < 0.05$).

3.3. Metallic magnetic particles

The unexposed lichens showed a relatively low mean $\chi = 1.9 \pm 0.2 \times 10^{-8}\ m^3\ kg^{-1}$, while χ of exposed samples was remarkably higher and decreased exponentially with distance from the highway ($R^2 = 0.96$, $p < 0.05$). In the "Day Plot", as the distance from the road increased the samples progressively shifted towards finer magnetic grain-sizes within the PSD range, thus approaching unexposed lichens (Fig. 4).

The FORC diagrams of selected samples (Fig. 5) were quite noisy due to the weak magnetic signal. They showed a progressive change from finer PSD features in the unexposed sample (a), to emerging MD characteristics peaked at Bc~0 for site 6 (b), up to prevailing MD magnetic properties at site 1 (c).

3.4. Pollutant associations

Correlation analysis showed strong and significant associations among traffic tracers. The correlation between Cr, Sb, and χ ranged from $r = 0.96–0.98$ (Fig. 6). Tire wear particles were most strongly correlated with χ ($r = 0.83$).

The normalized (over the maximum value) decay trend of Fe was consistently above those of χ and Sb, which were roughly overlapping, and TWP, which was the lowest (Fig. 7).

4. Discussion

This study demonstrated the suitability of the lichen *E. prunastri* for biomonitoring the deposition of airborne non-exhaust particles, at least under dry conditions. The high number of TWPs accumulated in lichen samples was consistent with the heavy vehicular traffic along Highway 401. A notable limitation of monitoring TWPs is the high rate of particles derived from road wear, embedded in tire fragments. Many studies merge tire and road wear particles (TRWP) since the contact between the tread and road during the driving process generates mixed particles (Baensch-Baltruschat et al., 2020; Kreider et al., 2010; Panko et al., 2013). The present study suffered from limitations linked to the estimation of TWP abundance, and for this reason, the number of TWPs was corrected for the proportion of mineral or organic particles derived from road surface or exhaust emissions (analytically determined using μ-FTIR). The exposure period occurred in the summer, a season characterized by elevated emissions of non-exhaust particles due to increased road surface temperatures, enhanced tire-road friction, and high traffic volumes (Vogelsang et al., 2019). The highest mass of TWPs was observed at Site 1 (5 m from the highway) and decreased with distance from the highway and this trend reflected the rapid deposition of coarse and heavy particles near the emission source, while finer particles were transported at least 150 m farther. An exponential decline of TWP with increasing distance from the highway indicated the strong

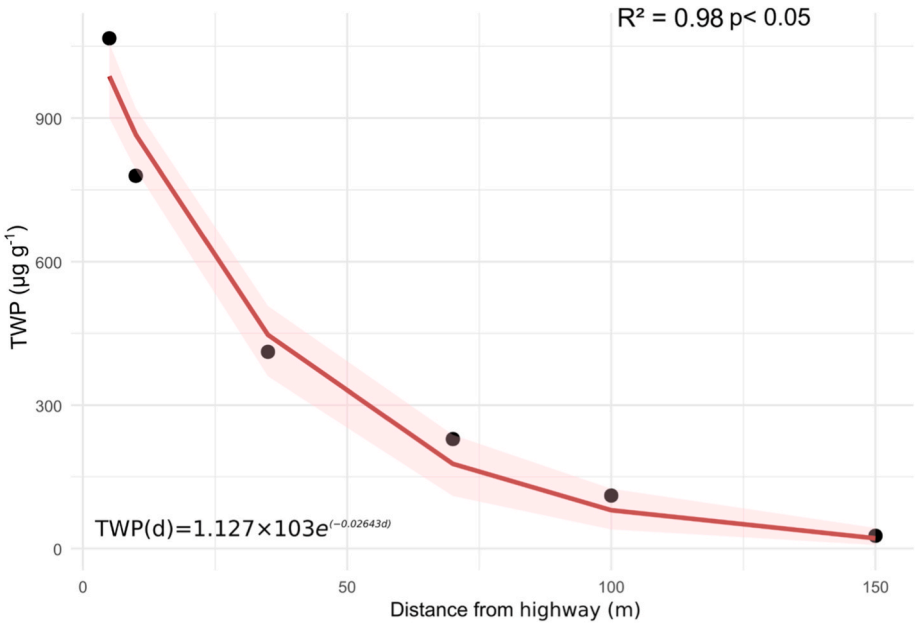

Fig. 2. Relationship between tire wear particle (TWP) mass accumulation (µg g^{-1}) by lichen transplants and distance (m) from Highway 401, Toronto, Canada.

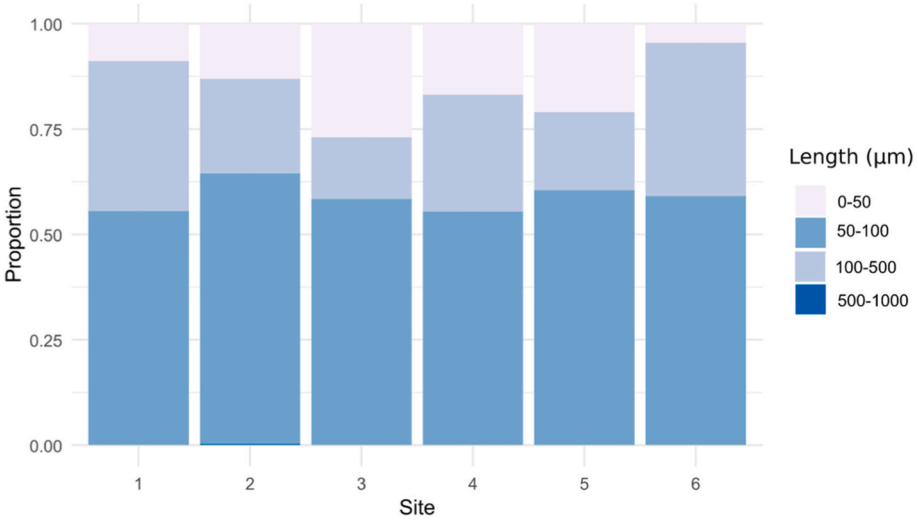

Fig. 3. Length range (µm) proportion of tire wear particles accumulated by lichen transplants at each of the six study sites (see Table 1).

Table 2
Concentration (µg g^{-1}, mean ± standard error) of potentially toxic elements accumulated by lichen transplants at each site (n = 3); values of unexposed (unexp) samples are also shown.

Site	Al	Ba	Cd	Cr	Cu	Fe	Mn	Sb	Zn
unexp	388 ± 33	10 ± 3	0.08 ± 0.00	0.7 ± 0.1	4.8 ± 0.2	292 ± 26	19 ± 1	0.07 ± 0.00	20 ± 1
1	409 ± 26	43 ± 3	0.15 ± 0.03	2.7 ± 0.2	8.7 ± 0.3	776 ± 50	33 ± 2	1.86 ± 0.18	381 ± 44
2	363 ± 35	36 ± 8	0.10 ± 0.01	2.3 ± 0.5	7.8 ± 1.2	681 ± 122	33 ± 3	1.50 ± 0.50	149 ± 59
3	352 ± 31	29 ± 3	0.13 ± 0.03	1.9 ± 0.3	7.6 ± 0.6	600 ± 89	35 ± 2	1.05 ± 0.18	94 ± 4
4	388 ± 23	24 ± 1	0.08 ± 0.0	1.8 ± 0.1	7.3 ± 0.1	544 ± 17	30 ± 1	0.75 ± 0.06	147 ± 57
5	363 ± 13	29 ± 8	0.07 ± 0.01	1.4 ± 0.1	6.7 ± 0.0	487 ± 24	27 ± 1	0.52 ± 0.01	225 ± 32
6	466 ± 12	16 ± 1	0.07 ± 0.01	1.2 ± 0.0	9.3 ± 0.9	411 ± 3	24 ± 1	0.38 ± 0.03	257 ± 74

influence of proximity to the source on traffic particulate deposition dynamics. In general, TWPs were largely deposited in proximity to the highway, with 47% of the total mass within the first 10 m. Despite methodological differences, absolute values and the decay rate (>90% by 150 m) of our study align well with other studies investigating atmospheric TWP deposition. In Frankfurt, Germany, airborne TWP mass concentrations declined from approximately 7.8 to 2.8 µg m^{-2} d^{-1} between 3.5 m and 30 m from a busy motorway (Weinbruch et al., 2025). Similarly, in Fribourg, Switzerland, TWPs decreased from 13.7 to 1.2 µg m^{-3} between 5 and 30 m from a highway (Gao et al., 2022). The high deposition of TWPs is also supported by the elevated accumulation of Zn, used as tire wear tracer (Hicks et al., 2021), which showed a tenfold

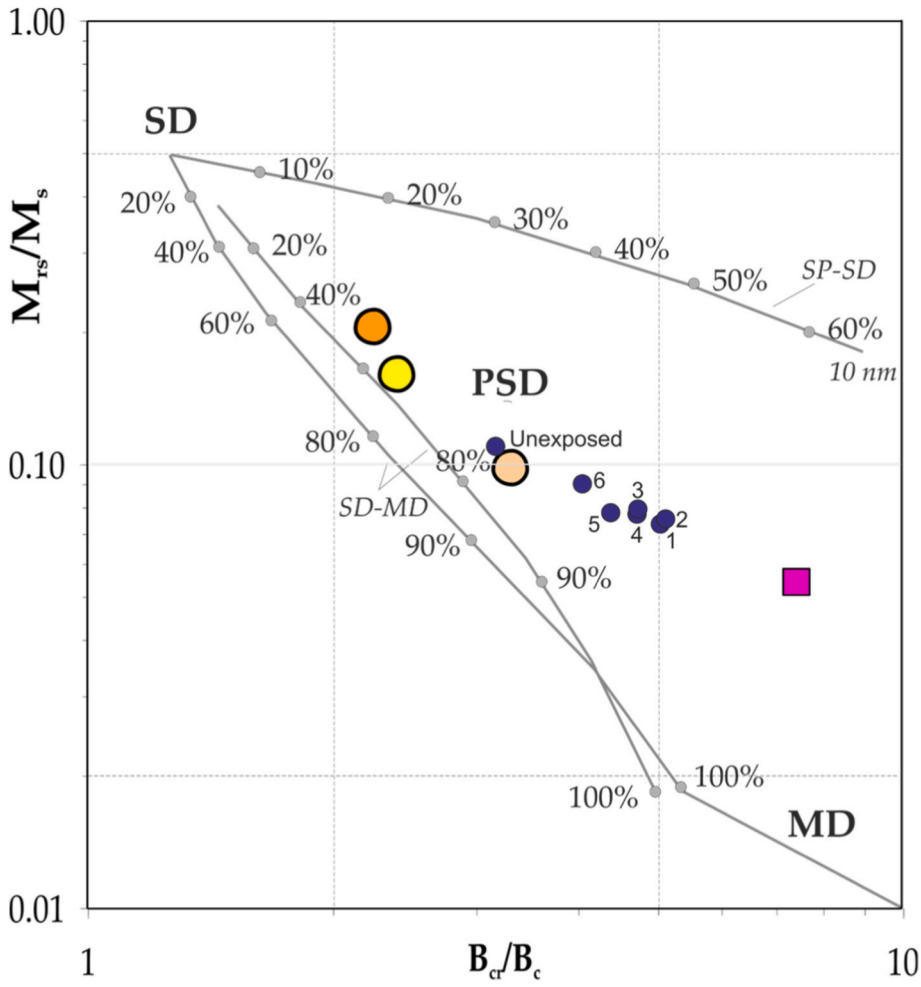

Fig. 4. Biologarithmic "Day Plot" of one selected lichen sample for site, along with the average points of fuel exhausts (orange, yellow and pink circles, respectively for gasoline, large diesel and diesel cars) and brake dust emissions (purple square) calculated from Sagnotti et al. (2009). The SD (single domain), PSD (pseudo-single domain) and MD (multidomain) fields and the theoretical mixing trends for SD-MD and SP-SD pure magnetite particles (SP, superparamagnetic) are from Dunlop (2002a, 2002b).

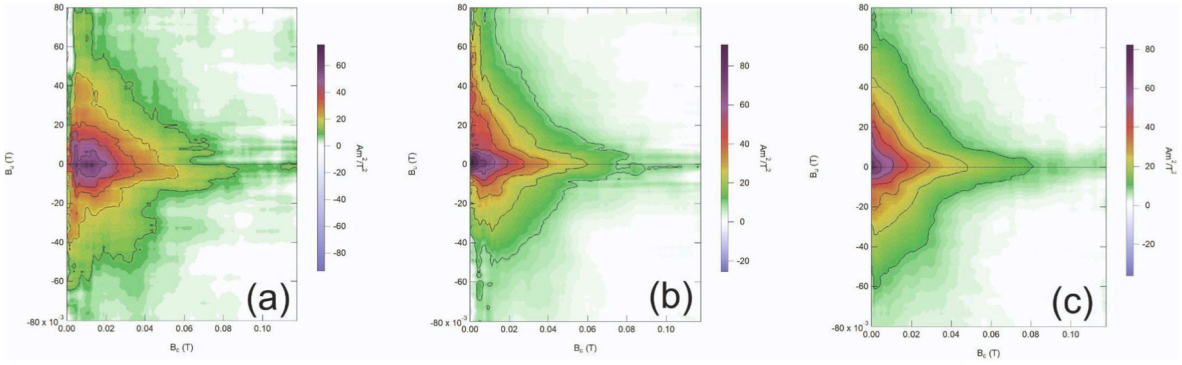

Fig. 5. First-order reversal curve (FORC) diagrams for unexposed (a), site 6 (b) and site 1 (c) samples (see Table 1).

increase compared with controls. However, the concentration of Zn may also have been influenced by leaching from the zinc-plated L-brackets used to deploy the bags.

No significant variation was found in the dimensional range along the transect, but the predominance of short particles (<100 μm) and ellipsoid or elongated morphologies is consistent with other studies investigating TWPs in urban areas (Dall'Osto et al., 2014).

The mixture of polymers detected, including rubber, PP, and PMMA, was consistent with findings from urban passive sampling campaigns (Järlskog et al., 2022). This variability in TWP composition was expected, as it depends on vehicle type, tire formulation, and road conditions. An all-season tire may contain about 30 types of synthetic rubbers along with natural rubbers, carbon black, polyester and nylon fibres, chemicals, waxes, oils, paints, and other minor components (Baumann and Ismeier, 1998).

The *E. prunastri* transplants were valuable detectors for a broad suite

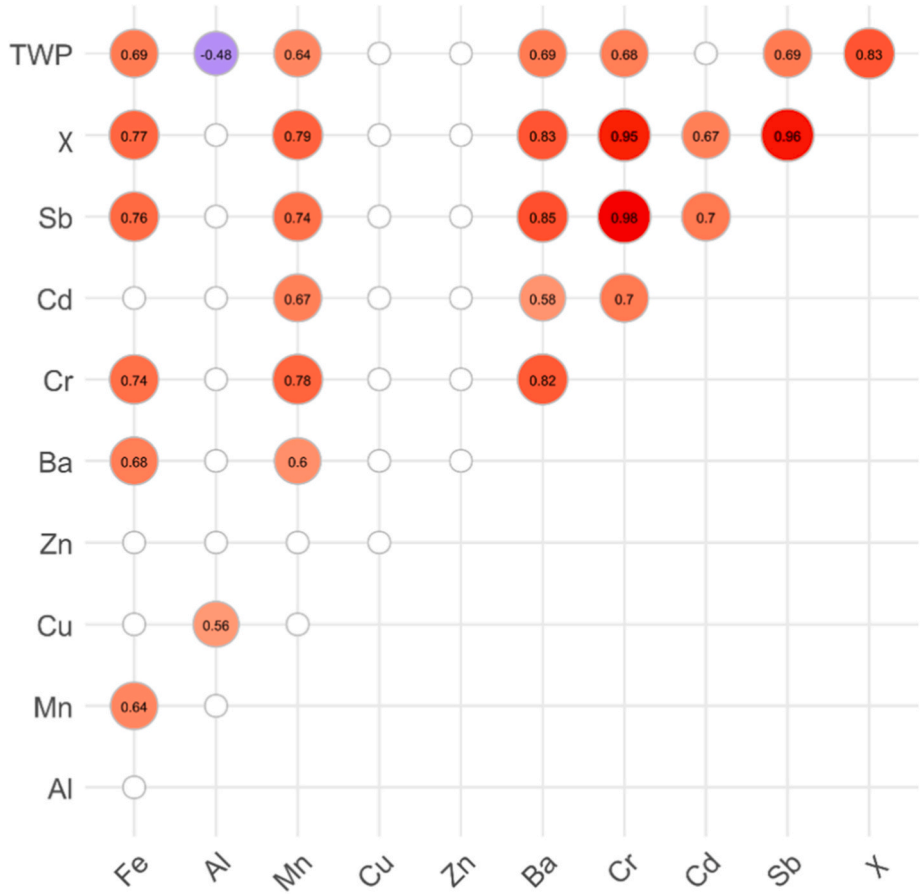

Fig. 6. Correlation plot between potentially toxic elements (μg g^{-1}), tire wear particles (TWP; μg g^{-1}) and magnetic susceptibility (χ). Only statistically significant ($p < 0.05$) correlations are shown.

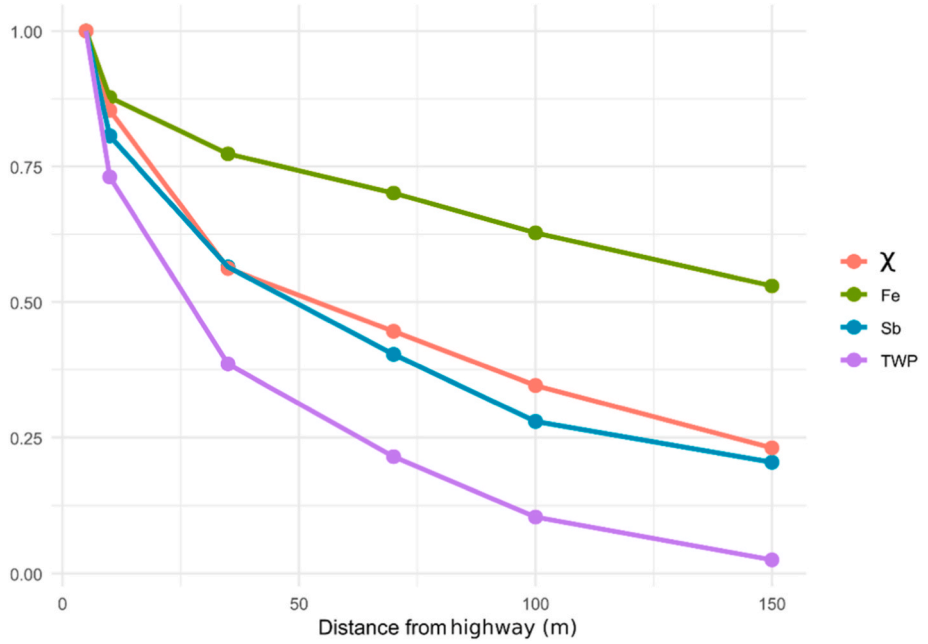

Fig. 7. Normalized decay of iron (Fe), antimony (Sb), magnetic susceptibility (χ), and tire wear particles (TWP) with distance (m) from Highway 401, Toronto, Canada.

of PTEs as well as MMPs and TWPs. The methodological framework aligned with recent lichen-based spatial monitoring efforts in European cities, considering both native species (Niepsch et al., 2024) and transplants (e.g., Winkler et al., 2020; Grifoni et al., 2024). These studies

demonstrate that small-scale, transplant-based designs may enable high-resolution contamination mapping. Compared to other studies that similarly employed *E. prunastri* for a two or three-month exposure period (Loppi and Paoli, 2015; Loppi et al., 2019; Paoli et al., 2019; Nannoni et al., 2015; Winkler et al., 2020, 2022; Grifoni et al., 2024, 2025b), our results showed a higher accumulation for key traffic tracers such as Fe and especially Sb.

In this study, lichens accumulated over 70% of the total Sb and χ of the transect within 35 m of the road, indicating a marked deposition gradient of non-exhaust emissions. This pattern was consistent with previous observations that reported similar spatial declines in Sb near roadways (Parviainen et al., 2020). Moreover, Szönyi et al. (2008) showed that χ values decrease to a magnetic background level 30 m away from high-traffic roads.

The Cu:Sb ratio is typically used as an indicator of brake wear emission (Sternbeck et al., 2002; Thorpe and Harrison, 2008), with values in the range 4.4–8 being indicative of brake wear, while crustal values are typically much higher, about 125:1 (Parviainen et al., 2020). Along our 150 m transect, the Cu:Sb ratio in lichen transplants showed a progressive increase, with values shifting from 5:1, 7:1, 8:1, 10:1, 13:1, 25:1, indicating a decay in the contribution of brake wear particles.

The range of magnetic susceptibility values in our samples (6–25 $\times$ 10^{-8} m^3 kg^{-1}; mean 14.4 $\times$ 10^{-8} m^3 kg^{-1}) was comparable to those observed in *P. furfuracea* transplants from a heavily polluted area near Rome (7.1–17.1 $\times$ 10^{-8} m^3 kg^{-1}; Winkler et al., 2019) and in *E. prunastri* samples collected across 25 sites in Milan, which averaged 15.68 $\times$ 10^{-8} m^3 kg^{-1} (Winkler et al., 2020).

The normalized decay sequence suggests that more than half of Fe was not connected to the same emissions source as MMPs and was likely of geogenic origin. Moreover, MMPs were strongly connected to Sb as they mostly originate from the same source, representing the non-exhaust emissions, whereas the fraction of TWPs was below, highlighting the tire wear component within the overall non-exhaust emissions.

The co-occurrence of high concentrations of Sb and Fe near the highway supports the use of these elements as traffic tracers, regardless of whether the vehicles are electric or fuel-powered, especially for brake and tire wearing (Grigoratos and Martini, 2014). Furthermore, the exponential decrease in χ along the transect was consistent with a progressive reduction in the deposition of ferromagnetic wear particles, found in brake dust (Matzka and Maher, 1999) and potentially embedded in TWPs. Moreover, the exponential decline in TWP mass with increasing distance from the highway is consistent with previous studies in Rome that demonstrated that the magnetic susceptibility of lichens decreases exponentially with distance from the road, when related to metallic emissions from vehicle brake abrasion (Winkler et al., 2022).

The strong correlations among the main traffic tracers (Fe, Mn, Cr, Sb), TWP and χ (Fig. 6) accumulated by lichen transplants suggested that these components of non-exhaust emissions deposited along the transect followed a similar pattern. Moreover, the correlation of TWPs with Sb and χ aligned with the coarse particulate matter distribution pattern, as confirmed by the "Day Plot" and the FORC diagrams, where the samples progressively acquired MD magnetic components with proximity to the road, consistent with the bioaccumulation of non-exhaust vehicular emissions (Sagnotti et al., 2009; Winkler et al., 2020).

5. Conclusions

This study used lichen transplants to investigate the occurrence and distribution patterns of traffic-related tire wear particles (TWPs), potentially toxic elements (PTEs), and magnetic particles (MMPs) along the busiest highway in Canada, with a special focus on their decay trends. Our results highlight that the lichen transplant technique is a valuable tool for detecting airborne traffic-related pollution, under dry conditions. A remarkable amount of TWP, PTEs and MMPs were observed within 35 m from the highway, followed by sharp exponential decay trends with distance. The correlation among TWP and non-exhaust emission tracers, such as Sb, Cr, and MMPs highlighted an impactful and shared source combining tire and brake wear components. Future studies should investigate the magnetic properties of tires to evaluate if magnetic susceptibility may be used as a rapid proxy for assessing the diffusion of TWPs.

CRediT authorship contribution statement

Lisa Grifoni: Writing – review & editing, Writing – original draft, Methodology, Investigation, Formal analysis, Data curation, Conceptualization. **Aldo Winkler:** Writing – review & editing, Supervision, Investigation, Funding acquisition, Formal analysis, Data curation. **Mehriban Jafarova:** Writing – review & editing, Methodology. **Lilla Spagnuolo:** Investigation. **Julian Aherne:** Writing – review & editing, Supervision, Methodology, Funding acquisition, Formal analysis, Data curation, Conceptualization. **Stefano Loppi:** Writing – review & editing, Supervision, Methodology, Investigation, Formal analysis, Data curation, Conceptualization.

Funding

This research was partly funded by INGV Project "Pianeta Dinamico" (Ministry of University and Research, Italy), research line 2023-2025 "CHIOMA", Cultural Heritage Investigations and Observations: a Multidisciplinary Approach. LG was partly funded by a Globalink Research Award during her time at Trent University.

Declaration of competing interest

The authors declare that they have no known competing financial interests or personal relationships that could have appeared to influence the work reported in this paper.

Acknowledgements

The authors would like to thank the Editor and the anonymous reviewers for their helpful comments provided during the peer-review process. In addition, the authors gratefully thank Dr Paul Helm, Ontario Ministry of the Environment Conservation and Parks, for his support in establishing the study transect.

References

Allen, S., Allen, D., Phoenix, V.R., et al., 2019. Atmospheric transport and deposition of microplastics in a remote mountain catchment. Nat. Geosci. 12, 339–344. https://doi.org/10.1038/s41561-019-0335-5.

Amato, F., Cassee, F.R., Denier van der Gon, H.A.C., Gehrig, R., Gustafsson, M., Hafner, W., Harrison, R.M., Jozwicka, M., Kelly, F.J., Moreno, T., Prevot, A.S.H., Schaap, M., Sunyer, J., Querol, X., 2014. Urban air quality: the challenge of traffic non-exhaust emissions. J. Hazard Mater. 275, 31–36. https://doi.org/10.1016/j.jhazmat.2014.04.053.

Baensch-Baltruschat, B., Kocher, B., Stock, F., Reifferscheid, G., 2020. Tire and road wear particles (TRWP) - a review of generation, properties, emissions, human health risk, ecotoxicity, and fate in the environment. In: Science of the Total Environment, 733. Elsevier B.V. https://doi.org/10.1016/j.scitotenv.2020.137823.

Baumann, W., Ismeier, M., 1998. Emissionen beim bestimmungsgemässen Gebrauch von Reifen. Kautsch. Gummi Kunstst. 51, 182–186.

Bertrim, C., Aherne, J., 2023. Moss bags as biomonitors of atmospheric microplastic deposition in urban environments. Biology 12 (2). https://doi.org/10.3390/biology12020149.

Boucher, J., Friot, D., 2017. Primary Microplastics in the Oceans: a Global Evaluation of Sources. IUCN, Gland, Switzerland, p. 43.

Brandt, J., Fischer, F., Kanaki, E., Enders, K., Labrenz, M., Fischer, D., 2021. Assessment of subsampling strategies in microspectroscopy of environmental microplastic samples. Front. Environ. Sci. 8, 579676.

Cercasov, V., Pantelică, A., Sălăgean, M., Caniglia, G., Scarlat, A., 2002. Comparative study of the suitability of three lichen species to trace-element air monitoring. Environ. Pollut. 119, 129–139. https://doi.org/10.1016/s0269-7491(01)00170-1.

Conti, M.E., Cecchetti, G., 2001. Biological monitoring: lichens as bioindicators of air pollution assessment — a review. Environ. Pollut. 114 (3), 471–492. https://doi.org/10.1016/S0269-7491(00)00224-4.
Cowger, W., Steinmetz, Z., Gray, A., Munno, K., Lynch, J., Hapich, H., Primpke, S., De Frond, H., Rochman, C., Herodotou, O., 2021. Microplastic spectral classification needs an open source community: open specy to the rescue. Anal. Chem. 93 (21), 7543–7548.
Dall'Osto, M., Beddows, D., Gietl, J., Yang, X., Harrison, R., Olatunbosun, O., 2014. Characteristics of tyre dust in polluted air: studies by single particle mass spectrometry (ATOFMS). Atmos. Environ. 94, 224–230. https://doi.org/10.1016/j.atmosenv.2014.05.026.
Day, R., Fuller, M., Schmidt, V.A., 1977. Hysteresis properties of titanomagnetites: grain-size and compositional dependence. Phys. Earth Planet. Inter. 13 (4), 260–267. https://doi.org/10.1016/0031-9201(77)90108-X.
Demková, L., Oboňa, J., Árvay, J., Michalková, J., Lošák, T., 2019. Biomonitoring road dust pollution along streets with various traffic densities. Pol. J. Environ. Stud. 28 (5), 3687–3696. https://doi.org/10.15244/pjoes/97354.
Dunlop, D.J., 2002a. Theory and application of the Day plot (M rs/M s versus H cr/H c) 1. Theoretical curves and tests using titanomagnetite data. J. Geophys. Res. Solid Earth 107 (B3). https://doi.org/10.1029/2001jb000486.
Dunlop, D.J., 2002b. Theory and application of the day plot (M rs/M s versus H cr/H c) 2. Application to data for rocks, sediments, and soils. J. Geophys. Res. Solid Earth 107 (B3). https://doi.org/10.1029/2001jb000487.
ECCC (Environment and Climate Change Canada), 2020. Historical climate data. Available online: https://climate.weather.gc.ca/historical_data/search_historic_data_e.html. (Accessed 7 May 2025).
Foroutan, H., Aryal, A., Craine, M., Rakha, H., 2025. Projecting airborne tire wear particle emissions in the United States in the era of electric vehicles. Sci. Total Environ. 967. https://doi.org/10.1016/j.scitotenv.2025.178848.
Fussell, J.C., Franklin, M., Green, D.C., Gustafsson, M., Harrison, R.M., Hicks, W., Kelly, F.J., Kishta, F., Miller, M.R., Mudway, I.S., Oroumiyeh, F., Selley, L., Wang, M., Zhu, Y., 2022. A review of road traffic-derived non-exhaust particles: emissions, physicochemical characteristics, health risks, and mitigation measures. Environ. Sci. Technol. 56 (11), 6813–6835. https://doi.org/10.1021/acs.est.2c01072.
Gao, Z., Cizdziel, J.v., Wontor, K., Clisham, C., Focia, K., Rausch, J., Jaramillo-Vogel, D., 2022. On airborne tire wear particles along roads with different traffic characteristics using passive sampling and optical microscopy, single particle SEM/EDX, and μ-ATR-FTIR analyses. Front. Environ. Sci. 10. https://doi.org/10.3389/fenvs.2022.1022697.
Giechaskiel, B., Grigoratos, T., Mathissen, M., Quik, J., Tromp, P., Gustafsson, M., Franco, V., Dilara, P., 2024. Contribution of road vehicle Tyre wear to microplastics and ambient air pollution. In: Sustainability (Switzerland), 16. Multidisciplinary Digital Publishing Institute (MDPI). https://doi.org/10.3390/su16020522. Issue 2.
Grifoni, L., Winkler, A., Lella, L. A. di, Buemi, L.P., Sgamellotti, A., Spagnuolo, L., Loppi, S., 2024. Magnetic and chemical biomonitoring of particulate matter at cultural heritage sites: the Peggy Guggenheim Collection case study (Venice, Italy). Environ. Adv. 15. https://doi.org/10.1016/j.envadv.2023.100455.
Grifoni, L., Jafarova, M., la Colla, N.S., Aherne, J., Raulli, A., Loppi, S., 2025a. Comparison of lichen and moss transplants for monitoring the deposition of airborne microfibers. Sustainability 17 (2). https://doi.org/10.3390/su17020537.
Grifoni, L., Winkler, A., Chaparro, M.A.E., di Lella, L.A., Marte, F., Sgamellotti, A., Spagnuolo, L., Tascon, M., Buitrago Posada, D., Marié, D.C., Scoccimarro, M., Loppi, S., 2025b. Magnetic and chemical biomonitoring with lichens and vascular plants for the preservation of cultural heritage: a case study at two museums in a megacity (Buenos Aires, Argentina). Sci. Total Environ. 988. https://doi.org/10.1016/j.scitotenv.2025.179836.
Grigoratos, T., Martini, G., 2014. Non-Exhaust Traffic Related Emissions - Brake and Tyre Wear PM Literature Review. Publications Office of the European Union.
Gulia, S., Shiva Nagendra, S.M., Khare, M., Khanna, I., 2015. Urban air quality management-A review. Atmos. Pollut. Res. 6 (2), 286–304. https://doi.org/10.5094/APR.2015.033.
Harrison, R.J., Feinberg, J.M., 2008. FORCinel: an improved algorithm for calculating first-order reversal curve distributions using locally weighted regression smoothing. G-cubed 9 (5). https://doi.org/10.1029/2008GC001987.
Hartmann, N.B., Hüffer, T., Thompson, R.C., Hassellöv, M., Verschoor, A., Daugaard, A. E., Rist, S., Karlsson, T., Brennholt, N., Cole, M., Herrling, M.P., Hess, M.C., Ivleva, N. P., Lusher, A.L., Wagner, M., 2019. Are we speaking the same Language? Recommendations for a definition and categorization framework for plastic debris. Environ. Sci. Technol. 53, 1039–1047. https://doi.org/10.1021/acs.est.8b05297.
Hicks, W., Beevers, S., Tremper, A.H., Stewart, G., Priestman, M., Kelly, F.J., Lanoisellé, M., Lowry, D., Green, D.C., 2021. Quantification of non-exhaust particulate matter traffic emissions and the impact of COVID-19 lockdown at London Marylebone road. Atmosphere 12 (2). https://doi.org/10.3390/atmos12020190.
Jafarova, M., Aherne, J., 2026. In search of an optimal moss transplant biomonitor for airborne microplastics: moss cubes. Environ. Pollut. 388. https://doi.org/10.1016/j.envpol.2025.127391.
Jafarova, M., Grifoni, L., Aherne, J., Loppi, S., 2023. Comparison of lichens and mosses as biomonitors of airborne microplastics. Atmosphere 14 (6). https://doi.org/10.3390/atmos14061007.
Järlskog, I., Jaramillo-Vogel, D., Rausch, J., Gustafsson, M., Strömvall, A.M., Andersson-Sköld, Y., 2022. Concentrations of tire wear microplastics and other traffic-derived non-exhaust particles in the road environment. Environ. Int. 170. https://doi.org/10.1016/j.envint.2022.107618.
Kole, J.P., Löhr, A.J., van Belleghem, F.G.A.J., Ragas, A.M.J., 2017. Wear and tear of tyres: a stealthy source of microplastics in the environment. In: International Journal of Environmental Research and Public Health, 14. MDPI. https://doi.org/10.3390/ijerph14101265. Issue 10.
Kreider, M.L., Panko, J.M., McAtee, B.L., Sweet, L.I., Finley, B.L., 2010. Physical and chemical characterization of tire-related particles: comparison of particles generated using different methodologies. Sci. Total Environ. 408, 652–659.
Leads, R.R., Weinstein, J.E., 2019. Occurrence of tire wear particles and other microplastics within the tributaries of the Charleston Harbor Estuary, South Carolina, USA. Mar. Pollut. Bull. 145, 569–582.
Limo, J., Paturi, P., Mäkinen, J., 2018. Magnetic biomonitoring with moss bags to assess stop-and-go traffic induced particulate matter and heavy metal concentrations. Atmos. Environ. 195, 187–195. https://doi.org/10.1016/j.atmosenv.2018.09.062.
Loppi, S., Paoli, L., 2015. Comparison of the trace element content in transplants of the lichen Evernia prunastri and in bulk atmospheric deposition: a case study from a low polluted environment (C Italy). Biologia (Poland) 70 (4), 460–466. https://doi.org/10.1515/biolog-2015-0053.
Loppi, S., Pacioni, G., Olivieri, N., di Giacomo, F., 1998. Accumulation of trace metals in the lichen Evernia prunastri transplanted at biomonitoring sites in Central Italy. Bryologist 101 (3), 451–454. https://doi.org/10.2307/3244187.
Loppi, S., Corsini, A., Paoli, L., 2019. Estimating environmental contamination and element deposition at a urban area of Central Italy. Urban Sci. 3, 76. https://doi.org/10.3390/urbansci3030076.
Loppi, S., Roblin, B., Paoli, L., Aherne, J., 2021. Accumulation of airborne microplastics in lichens from a landfill dumping site (Italy). Sci. Rep. 11 (1). https://doi.org/10.1038/s41598-021-84251-4.
Matzka, J., Maher, B.A., 1999. Magnetic biomonitoring of roadside tree leaves: identi"cation of spatial and temporal variations in vehicle-derived particulates. Atmos. Environ. 33.
Ministry of Transportation of Ontario, 2021. Traffic Volume Data: Annual Average Daily Traffic (AADT) for Provincial Highways. Government of Ontario.
Nannoni, F., Santolini, R., Protano, G., 2015. Heavy element accumulation in Evernia prunastri lichen transplants around a municipal solid waste landfill in central Italy. Waste Manag. 43, 353–362. https://doi.org/10.1016/j.wasman.2015.06.013.
Niepsch, D., Clarke, L.J., Jones, R.G., Tzoulas, K., Cavan, G., 2024. Lichen biomonitoring to assess spatial variability, potential sources and human health risks of polycyclic aromatic hydrocarbons (PAHs) and airborne metal concentrations in Manchester (UK). Environ. Monit. Assess. 196 (4). https://doi.org/10.1007/s10661-024-12522-4.
Panko, J.M., Chu, J., Kreider, M.L., Unice, K.M., 2013. Measurement of airborne concentrations of tire and road wear particles in urban and rural areas of France, Japan, and the United States. Atmos. Environ. 72, 192–199.
Panko, J., Kreider, M., Unice, K., 2018. Chapter 7 - review of tire wear emissions: a review of tire emission measurement studies: identification of gaps and future needs. Non-Exhaust Emissions. Academic Press, pp. 147–160. https://doi.org/10.1016/B978-0-12-811770-5.00007-8.
Paoli, L., Fačkovcová, Z., Maccelli, C., Guttová, A., Kresáňová, K., Loppi, S., 2019. Evernia goes to school: bioaccumulation of heavy metals and photosynthetic performance in lichen transplants exposed indoors and outdoors in public and private environments. Plants 8, 125. https://doi.org/10.3390/plants8050125.
Parmar, T.K., Rawtani, D., Agrawal, Y.K., 2016. Bioindicators: the natural indicator of environmental pollution. Front. Life Sci. 9 (2), 110–118. https://doi.org/10.1080/21553769.2016.1162753.
Parviainen, A., Papaslioti, E.M., Casares-Porcel, M., Garrido, C.J., 2020. Antimony as a tracer of non-exhaust traffic emissions in air pollution in Granada (S Spain) using lichen bioindicators. Environ. Pollut. 263. https://doi.org/10.1016/j.envpol.2020.114482.
Pike, C.R., Roberts, A.P., Verosub, K.L., 1999. Characterizing interactions in fine magnetic particle systems using first order reversal curves. J. Appl. Phys. 85 (9), 6660–6667. https://doi.org/10.1063/1.370176.
R Core Team, 2025. R: a Language and Environment for Statistical Computing. R Foundation for Statistical Computing. https://www.r-project.org/.
Roberts, A.P., Pike, C.R., Verosub, K.L., 2000. First-order reversal curve diagrams: a new tool for characterizing the magnetic properties of natural samples. J. Geophys. Res. Solid Earth 105 (B12), 28461–28475. https://doi.org/10.1029/2000jb900326.
Roblin, B., Aherne, J., 2020. Moss as a biomonitor for the atmospheric deposition of anthropogenic microfibres. Sci. Total Environ. 715. https://doi.org/10.1016/j.scitotenv.2020.136973.
Sagnotti, L., Taddeucci, J., Winkler, A., Cavallo, A., 2009. Compositional, morphological, and hysteresis characterization of magnetic airborne particulate matter in Rome, Italy. Geochem. Geophys. Geosyst. 10 (8). https://doi.org/10.1029/2009GC002563.
Sternbeck, J., Sjödin, Å., Andreasson, K., 2002. Metal emissions from road traffic and the influence of resuspension results from two tunnel studies. Atmos. Environ. 36, 4735e4744.
Szönyi, M., Sagnotti, L., Hirt, A.M., 2008. A refined biomonitoring study of airborne particulate matter pollution in Rome, with magnetic measurements on quercus ilex tree leaves. Geophys. J. Int. 173, 127–141. https://doi.org/10.1111/j.1365-246X.2008.03715.x.
Theophilo, C.Y.S., Ribeiro, A.P., Moreira, E.G., et al., 2021. Biomonitoring as a nature-based solution to assess atmospheric pollution and impacts on public health. Bull. Environ. Contam. Toxicol. 107, 29–36. https://doi.org/10.1007/s00128-021-03205-8.
Thorpe, A., Harrison, R.M., 2008. Sources and properties of non-exhaust particulate matter from road traffic: A review. Sci. Total Environ. 400, 270–282. https://doi.org/10.1016/j.scitotenv.2008.06.007.
Vogelsang, C., Lusher, A., Dadkhah, M.E., Sundvor, I., Umar, M., Ranneklev, S.B., et al., 2019. Microplastics in Road dust–characteristics, Pathways and Measures. NIVA-rapport.

Weinbruch, S., Matthies, J., Zou, L., Kandler, K., Ebert, M., Bigalke, M., 2025. Deposition rates and air concentrations of tire and road wear particles near a motorway in Germany. Atmos. Environ. 352. https://doi.org/10.1016/j.atmosenv.2025.121228.

Winkler, A., Contardo, T., Vannini, A., Sorbo, S., Basile, A., Loppi, S., 2020. Magnetic emissions from brake wear are the major source of airborne particulate matter bioaccumulated by lichens exposed in Milan (Italy). Appl. Sci. 10 (6). https://doi.org/10.3390/app10062073.

Winkler, A., Caricchi, C., Guidotti, M., Owczarek, M., Macrì, P., Nazzari, M., Amoroso, A., Di Giosa, A., Listrani, S., 2019. Combined magnetic, chemical and morphoscopic analyses on lichens from a complex anthropic context in Rome, Italy. Sci. Total Environ. 690, 1355–1368. https://doi.org/10.1016/j.scitotenv.2019.06.526.

Winkler, A., Contardo, T., Lapenta, V., Sgamellotti, A., Loppi, S., 2022. Assessing the impact of vehicular particulate matter on cultural heritage by magnetic biomonitoring at Villa Farnesina in Rome, Italy. Sci. Total Environ. 823. https://doi.org/10.1016/j.scitotenv.2022.153729.